

79992-27-1; VO(hfac)<sub>2</sub>·VI, 79992-28-2; Cu(hfac)<sub>2</sub>·VI, 79992-29-3; VO(tfac)<sub>2</sub>·VII, 79992-30-6; VO(hfac)<sub>2</sub>·VII, 79992-31-7; Cu(hfac)<sub>2</sub>·VII, 79992-32-8; VO(tfac)<sub>2</sub>·VIII, 80010-10-2; VO(hfac)<sub>2</sub>·VIII, 79992-33-9; Cu(hfac)<sub>2</sub>·VIII, 79992-34-0; VO(tfac)<sub>2</sub>·IX, 79992-35-1; VO(hfac)<sub>2</sub>·IX, 79992-36-2; Cu(hfac)<sub>2</sub>·IX, 79992-37-3; VO(tfac)<sub>2</sub>·X, 79992-38-4; VO(hfac)<sub>2</sub>·X, 79992-39-5; Cu(hfac)<sub>2</sub>·X, 79992-40-8; VO(tfac)<sub>2</sub>·XI, 79992-41-9; VO(hfac)<sub>2</sub>·XI, 79992-42-0; Cu(hfac)<sub>2</sub>·XI,

79992-43-1; 2,2,5,5-tetramethyl-1-oxypyrrolinyl-3-carboxylic acid chloride, 13810-21-4; 2,2,6,6-tetramethyl-1-oxo-1,2,5,6-tetrahydropyridinyl-4-carboxylic acid chloride, 79991-45-0; 2,2,5,5-tetramethyl-1-oxypyrrolidinyl-3-carboxylic acid chloride, 61593-19-9; 4-hydroxy-2,2,6,6-tetramethyl-1-oxypiperidine, 2226-96-2; 4-aminopyridine, 504-24-5; 3-aminopyridine, 462-08-8; isonicotinic acid, 55-22-1; 4-hydroxypyridine, 5382-16-1.

Contribution from the Institut für Anorganische, Analytische und Physikalische Chemie, Universität Bern, CH-3012 Bern, Switzerland

## Optical Spectroscopy of [(NH<sub>3</sub>)<sub>4</sub>Cr(OH)<sub>2</sub>Cr(NH<sub>3</sub>)<sub>4</sub>]<sup>4+</sup> and [(en)<sub>2</sub>Cr(OH)<sub>2</sub>Cr(en)<sub>2</sub>]<sup>4+</sup>

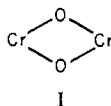
SILVIO DECURTINS, HANS U. GÜDEL,\* and ANDREAS PFEUTI

Received March 18, 1981

The compounds [(en)<sub>2</sub>Cr(OH)<sub>2</sub>Cr(en)<sub>2</sub>]Cl<sub>4</sub>·2H<sub>2</sub>O, [(en)<sub>2</sub>Cr(OH)<sub>2</sub>Cr(en)<sub>2</sub>]Br<sub>4</sub>·2H<sub>2</sub>O, [(NH<sub>3</sub>)<sub>4</sub>Cr(OH)<sub>2</sub>Cr(NH<sub>3</sub>)<sub>4</sub>]Cl<sub>4</sub>·4H<sub>2</sub>O, and [(NH<sub>3</sub>)<sub>4</sub>Cr(OH)<sub>2</sub>Cr(NH<sub>3</sub>)<sub>4</sub>]Br<sub>4</sub>·4H<sub>2</sub>O were prepared, structurally characterized, and studied by optical single-crystal absorption spectroscopy. Common to all the compounds is a strong linear dichroism. This is the result of unusually intense spin-allowed d-d transitions polarized perpendicular to the I plane. This behavior is rationalized in terms of an intensity stealing mechanism from ligand → e<sub>g</sub> charge-transfer transitions. The exchange coupling is antiferromagnetic with parameters 2J on the order -1 cm<sup>-1</sup> in the [NH<sub>3</sub>] compounds and -31 and -30 cm<sup>-1</sup> in [en]Cl<sub>4</sub>·2H<sub>2</sub>O and [en]Br<sub>4</sub>·2H<sub>2</sub>O, respectively. These differences in magnetic properties are accompanied by differences in the spectroscopic behavior, and they have a common physical origin. In the [en] compounds the hydrogen atom lies more or less in the plane defined by I, while in the [NH<sub>3</sub>] salts it is forced out of this plane by hydrogen bonding. The p<sub>x</sub> orbital (x is perpendicular to I) on the bridging oxygen is fully available for π bonding to the chromium in the [en] compounds, while in the [NH<sub>3</sub>] compounds it is not. The superexchange pathway through p<sub>x</sub>(O) is thus blocked to a large extent in [NH<sub>3</sub>]Cl<sub>4</sub>·4H<sub>2</sub>O and [NH<sub>3</sub>]Br<sub>4</sub>·4H<sub>2</sub>O, and the ligand field felt by chromium is sufficiently altered to produce significant changes in the optical spectra.

### Introduction

Structural and magnetochemical properties of di-μ-hydroxo-bridged chromium(III) species are being intensively studied at present.<sup>1-4</sup> One of the main aims is to establish a correlation between structural properties and the magnitude of the exchange splitting of the ground state. Pedersen and co-workers were the first to point to the importance of the position of the hydrogen atom in these structural-magnetic correlations.<sup>1</sup> Several examples of both dinuclear and tetranuclear complexes exhibiting di-μ-hydroxo bridging show that a correlation exists between the magnitude of the exchange parameter and the displacement of the hydrogen atom out of the



plane.<sup>4,5</sup> If the main superexchange pathway is through π bonding via the p<sub>x</sub> orbital (coordinate system Figure 1) at the oxygen, such a correlation is most easily understood.

An analysis of electronically excited <sup>2</sup>E states, from which, at least in principle, the dominant contributions to the net exchange can be deduced, has not been done for di-μ-hydroxo-bridged chromium(III) species. In a systematic study of a large number of complexes by single-crystal absorption spectroscopy, we found that compounds containing [(en)<sub>2</sub>Cr(OH)<sub>2</sub>Cr(en)<sub>2</sub>]<sup>4+</sup> (abbreviated [en] in the following)

and [(NH<sub>3</sub>)<sub>4</sub>Cr(OH)<sub>2</sub>Cr(NH<sub>3</sub>)<sub>4</sub>]<sup>4+</sup> (abbreviated [NH<sub>3</sub>]) generally exhibited much more fine structure in the region of spin-forbidden transitions than any of the other complexes. Focusing our attention on [en] and [NH<sub>3</sub>] compounds, we found a new modification of [NH<sub>3</sub>]Cl<sub>4</sub>·4H<sub>2</sub>O and [NH<sub>3</sub>]Br<sub>4</sub>·4H<sub>2</sub>O. In this modification, the antiferromagnetic coupling of the chromium(III) centers in the [NH<sub>3</sub>] complexes is very weak with 2J on the order of -1 cm<sup>-1</sup>.<sup>6</sup> In the corresponding [en] compounds, on the other hand, the exchange coupling is stronger by more than 1 order of magnitude (Table I).<sup>2</sup> In their optical spectroscopic behavior, [en]Cl<sub>4</sub>·2H<sub>2</sub>O and [en]Br<sub>4</sub>·2H<sub>2</sub>O on the one hand and [NH<sub>3</sub>]Cl<sub>4</sub>·4H<sub>2</sub>O and [NH<sub>3</sub>]Br<sub>4</sub>·4H<sub>2</sub>O on the other show close similarities as well as marked differences. We decided to explore the physical origins of these interesting magnetic and spectroscopic phenomena in detail. In the present paper the general spectroscopic properties are discussed and related to structural and exchange effects.

### Experimental Section

(1) **Preparation, Structure, and Morphology.** [(en)<sub>2</sub>Cr(OH)<sub>2</sub>Cr(en)<sub>2</sub>]Cl<sub>4</sub>·2H<sub>2</sub>O and [(en)<sub>2</sub>Cr(OH)<sub>2</sub>Cr(en)<sub>2</sub>]Br<sub>4</sub>·2H<sub>2</sub>O. The compounds were prepared following literature procedures.<sup>7</sup> Single crystals large enough for optical and spectroscopic investigation were obtained by slow diffusion of the counterion through a dialyze membrane into a saturated solution of the complex. Shiny red-violet crystals with well-developed faces and edge lengths up to 0.5 mm were thus obtained. Both compounds are isomorphous and crystallize in the triclinic system, space group P1̄. The grown crystal faces were found to be {100}, {010}, and {001} from Bürger precession X-ray photographs.

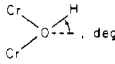
[(NH<sub>3</sub>)<sub>4</sub>Cr(OH)<sub>2</sub>Cr(NH<sub>3</sub>)<sub>4</sub>]Br<sub>4</sub>·4H<sub>2</sub>O was prepared following a literature method.<sup>7</sup>

[(NH<sub>3</sub>)<sub>4</sub>Cr(OH)<sub>2</sub>Cr(NH<sub>3</sub>)<sub>4</sub>]Cl<sub>4</sub>·4H<sub>2</sub>O was prepared from the perchlorate salt.<sup>7</sup> A 1.4-mmol sample of [(NH<sub>3</sub>)<sub>4</sub>Cr(OH)<sub>2</sub>Cr(NH<sub>3</sub>)<sub>4</sub>](ClO<sub>4</sub>)<sub>4</sub>·2H<sub>2</sub>O is added to 5 mL of a saturated (at room tem-

- (1) (a) Josephsen, J.; Pedersen, E. *Inorg. Chem.* 1977, 16, 2534. (b) Michelsen, K.; Pedersen, E. *Acta Chem. Scand., Ser. A* 1978, A32, 847.
- (2) Beutler, A.; Güdel, H. U.; Snellgrove, T. R.; Chapuis, G.; Schenk, K. *J. Chem. Soc., Dalton Trans.* 1979, 983.
- (3) Cline, S. J.; Kallesøe, S.; Pedersen, E.; Hodgson, D. J. *Inorg. Chem.* 1979, 18, 796.
- (4) Pedersen, E., private communication.
- (5) Güdel, H. U.; Hauser, U. *J. Solid State Chem.* 1980, 35, 230.

- (6) Decurtins, S.; Güdel, H. U., to be submitted for publication.
- (7) Springborg, J.; Schäffer, C. E. *Inorg. Synth.* 1978, 18, 75.

Table I. Structural and Magnetic Properties

		$2J,^a \text{ cm}^{-1}$	ref
$[(\text{en})_2\text{Cr}(\text{OH})_2\text{Cr}(\text{en})_2] \text{Cl}_4 \cdot 2\text{H}_2\text{O}$	6 (2)	-31 (1)	2
$[(\text{en})_2\text{Cr}(\text{OH})_2\text{Cr}(\text{en})_2] \text{Br}_4 \cdot 2\text{H}_2\text{O}$	6 (2)	-30 (1)	2
$[(\text{NH}_3)_4\text{Cr}(\text{OH})_2\text{Cr}(\text{NH}_3)_4] \text{Cl}_4 \cdot 4\text{H}_2\text{O}$	>30, <63	-1.2 (0.2)	6
$[(\text{NH}_3)_4\text{Cr}(\text{OH})_2\text{Cr}(\text{NH}_3)_4] \text{Br}_4 \cdot 4\text{H}_2\text{O}$	>30, <63	-0.6 (0.3)	6

<sup>a</sup>  $2J$  is the ground-state exchange parameter.

Table II. Crystal Data for the New Modifications of the  $[(\text{NH}_3)_4]$  Compounds<sup>a</sup>

	$[(\text{NH}_3)_4\text{Cr}(\text{OH})_2\text{Cr}(\text{NH}_3)_4] \text{Br}_4 \cdot 4\text{H}_2\text{O}$	$[(\text{NH}_3)_4\text{Cr}(\text{OH})_2\text{Cr}(\text{NH}_3)_4] \text{Cl}_4 \cdot 4\text{H}_2\text{O}$	$[(\text{NH}_3)_4\text{Co}(\text{OH})_2\text{Co}(\text{NH}_3)_4] \text{Cl}_4 \cdot 4\text{H}_2\text{O}$	
			a	b
$a/\text{Å}$	6.92 (3)	6.67 (3)	6.66 (2)	6.72 (3)
$b/\text{Å}$	8.11 (3)	7.87 (3)	7.82 (2)	7.76 (3)
$c/\text{Å}$	10.44 (3)	10.23 (3)	10.04 (2)	10.06 (3)
$\alpha/\text{deg}$	91.3 (2)	92.4 (2)	92.2 (2)	92.8 (2)
$\beta/\text{deg}$	107.4 (2)	106.5 (2)	106.8 (2)	106.3 (2)
$\gamma/\text{deg}$	107.2 (2)	106.5 (2)	106.6 (2)	106.5 (2)
$V/\text{Å}^3$	530.4	489.4	475.5	469.2
$Z$	1	1	1	1
space group	$P\bar{1}$	$P\bar{1}$	$P\bar{1}$	$P\bar{1}$
$D_m/\text{g cm}^{-3}$	2.05 (5)	1.61 (5)	1.74	1.78 (1)
$D_c/\text{g cm}^{-3}$	2.08	1.65	1.76	1.78

<sup>a</sup> Literature data of the related  $[(\text{NH}_3)_4\text{Co}(\text{OH})_2\text{Co}(\text{NH}_3)_4] \text{Cl}_4 \cdot 4\text{H}_2\text{O}$  are included for comparison: (a) ref 9; (b) ref 8.

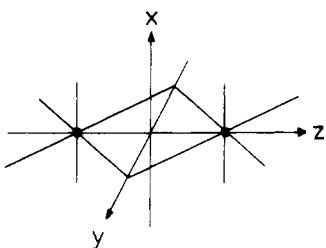


**Figure 1.** Schematic representation of the dimeric chromium complex in idealized  $D_{2h}$  symmetry and definition of the molecular coordinate frame.

perature) solution of ammonium chloride, and the suspension is cooled in an ice bath under thorough stirring for  $3/4$  h. The crude solid is filtered off, washed with ethanol, and dried in air. For purification, 0.6 g of the product is dissolved in 2.5 mL of 0.01 M HCl and, after filtration, reprecipitated by the addition of 5 mL of saturated  $\text{NH}_4\text{Cl}$  solution, while stirring and cooling in ice. The polycrystalline product is isolated as above with a yield of 0.4 g. Anal. Calcd: Cr, 21.30; Cl, 29.05; N, 22.96; H, 7.02. Found: Cr, 21.4; Cl, 28.3; N, 23.0; H, 6.5. Crystals of both compounds were grown by the dialyzation technique at 7 °C. After 4 h, perfect red crystals with edge lengths up to 1 mm were obtained. Crystal structures of the compounds have not been published. They appear to occur in more than one modification. Pedersen, using the same preparative procedure, obtained a different modification from ours.<sup>4</sup> From X-ray precession photographs we determined the triclinic unit cells and space groups in Table II. The chloride and bromide salts are likely to be isostructural. From the very close similarity of unit cells, we conclude that the chloride salt is isomorphous with  $[(\text{NH}_3)_4\text{Co}(\text{OH})_2\text{Co}(\text{NH}_3)_4] \text{Cl}_4 \cdot 4\text{H}_2\text{O}$ , the structure of which has been determined.<sup>8,9</sup> Crystals with {100}, {010}, and {001} faces were used for the optical and spectroscopic work.

**(2) Optical Investigation.** All the crystals were examined under the polarizing microscope. Since they crystallize in the triclinic system, a knowledge of their optical properties is necessary in order to devise meaningful spectroscopic experiments. For  $[\text{en}]\text{Br}_4 \cdot 2\text{H}_2\text{O}$  the orientation of the optical indicatrix as well as its wavelength and temperature dispersion were determined. Standard methods of mineralogy and optical crystallography were used.<sup>10-12</sup> Refractive indices were

Table III. Refractive Indices of  $[(\text{en})_2\text{Cr}(\text{OH})_2\text{Cr}(\text{en})_2] \text{Br}_4 \cdot 2\text{H}_2\text{O}$ 

crystal face	extinction direction <sup>a</sup>	refractive index
{010}	$E_1$	1.674 (2)
	$E_2$	1.662 (2)
{100}	$E_3$	1.678 (2)
	$E_4$	1.646 (2)
{001}	$E_5$	1.643 (2)
	$E_6$	1.671 (2)

axes <sup>b</sup>	refractive index	axes <sup>b</sup>	refractive index
X	1.643 (2)	Z	1.678 (2)
Y	1.672 (2)		

<sup>a</sup> Extinction directions are defined in Figure 2. <sup>b</sup> X, Y, and Z are the principal axes of the optical indicatrix.

determined by the immersion method.<sup>12</sup>

**(3) Spectroscopic Measurements.** Single-crystal absorption spectra were measured on a Cary 17 spectrometer. Because of the small size of the crystals (down to 20  $\mu\text{m}$  thick and 200- $\mu\text{m}$  edge length) a focusing device containing a pair of reflecting objectives (Ealing Beck) was introduced into the sample beam.<sup>13</sup> The samples were cooled by helium gas flow-tube technique. A red-sensitive GaAs photodetector was used. The light was polarized by a pair of Glan-Taylor prisms.

Light was propagating perpendicular to the natural {100}, {010}, and {001} faces with the electric vector parallel to the extinction directions. Figure 2 shows the relative orientation of unit cells, extinction directions, and molecules in the relevant projections.

## Results

**(1) Optical Properties.** No temperature dispersion of the optical indicatrix was found for  $[\text{en}]\text{Br}_4 \cdot 2\text{H}_2\text{O}$  between 77 and 293 K. Extinction directions vary by less than 2° in the {100} and {010} faces between 440 and 650 nm. Dispersion effects may therefore be safely neglected.

In Figure 1 we define a molecular coordinate system x, y, z. Since there is only one molecule per unit cell, all the molecules have the same orientation in the crystal. X, Y, and Z define the principal axes of the optical indicatrix. Within

(8) Prout, C. K. *J. Chem. Soc.* **1962**, 4429.  
 (9) Vannerberg, N. G. *Acta Chem. Scand.* **1963**, 17, 85.  
 (10) Bloss, F. D. "An Introduction to the Methods of Optical Crystallography"; Holt, Rinehart and Winston: New York, 1961; p 154.

(11) Waldmann, H. *Schweiz. Mineral. Petrogr. Mitt.* **1947**, 27, 472.  
 (12) Kleber, W. "Einführung in die Kristallographie"; VEB Verlag Technik: Berlin, 1974; p 288.  
 (13) Ferguson, J.; Orr, W. *Rev. Sci. Instrumen.* **1973**, 44, 225.

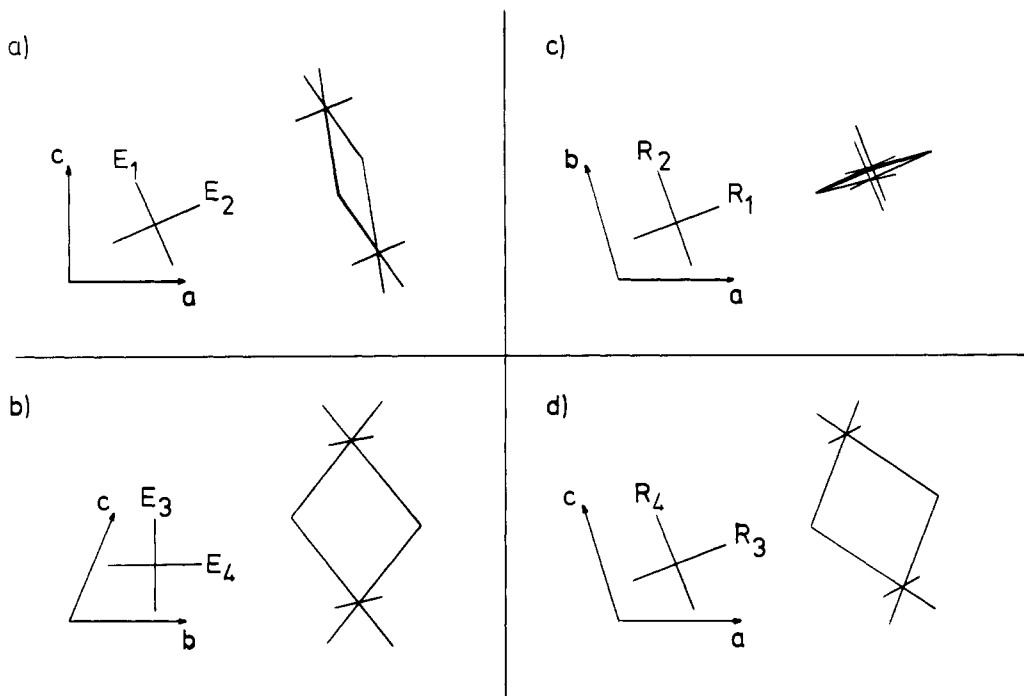


**Figure 2.** Molecular projections on crystal faces: (a) [en] {010}; (b) [en] {100}; (c) [NH<sub>3</sub>] {001}; (d) [NH<sub>3</sub>] {010}. Extinction directions are designated E<sub>1</sub>...E<sub>4</sub> for [en] and R<sub>1</sub>...R<sub>4</sub> for [NH<sub>3</sub>], respectively.

**Table IV.** Squares of Projections of Molecular Symmetry Axes on Extinction Directions (As Defined in Figure 2)<sup>a</sup>

	x	y	z
[en]Br <sub>4</sub> ·2H <sub>2</sub> O and [en]Cl <sub>4</sub> ·2H <sub>2</sub> O			
E <sub>1</sub>	0.02	0.04	0.94
E <sub>2</sub>	0.94	0.06	0.00
E <sub>4</sub>	0.11	0.89	0.00
[NH <sub>3</sub> ]Br <sub>4</sub> ·4H <sub>2</sub> O and [NH <sub>3</sub> ]Cl <sub>4</sub> ·4H <sub>2</sub> O			
R <sub>2</sub>	0.95	0.05	0.00
R <sub>3</sub>	0.03	0.95	0.02
R <sub>4</sub>	0.00	0.03	0.97

<sup>a</sup> Structural parameters from the isostructural  $[(\text{NH}_3)_4\text{Co}(\text{OH})_2\text{Co}(\text{NH}_3)_4 \cdot 4\text{H}_2\text{O}]^{8,9}$  were used for the calculation of the [NH<sub>3</sub>] projections.

experimental accuracy ( $\pm 2^\circ$ ), Z and z are parallel in [en]-Br<sub>4</sub>·2H<sub>2</sub>O. The rotation angle between (x,y) and (X,Y) is 58°. The behavior is optically negative.<sup>10</sup> The refractive indices are listed in Table III.

Due to the special orientation of the indicatrix with respect to molecular symmetry axes, absorption spectra polarized along the extinction directions are dominated by one molecular symmetry component. Results are summarized in Figure 2 and Table IV.

When viewed perpendicular to {010}, the [en] compounds show a pronounced dichroism. With the electric vector parallel E<sub>1</sub> (Figure 2), which corresponds to  $\vec{E} \parallel z$ , the color is light pink. With  $\vec{E}$  along E<sub>2</sub>, corresponding approximately to  $\vec{E} \parallel x$ , the color is dark red. The crystals do not show a strong dichroism in the {100} plane, and the color is light pink. A strong x-polarized absorption is responsible for the strongly dichroic behavior.

A completely analogous dichroism is observed in the [NH<sub>3</sub>] compounds when viewed perpendicular to the {001} plane. Again the intense absorption is x polarized.

**(2) Spectra.** Figure 3 shows the results of single-crystal absorption experiments on [en]Br<sub>4</sub>·2H<sub>2</sub>O. The corresponding chloride spectrum is very similar. The strong dichroism observed optically is the result of an unusually intense x-polarized component of  ${}^4A_2 \rightarrow {}^4T_2$ . The  ${}^4A_2 \rightarrow {}^1T_1$  is also predominantly x polarized. Three components of the  ${}^4T_2$  transition separated

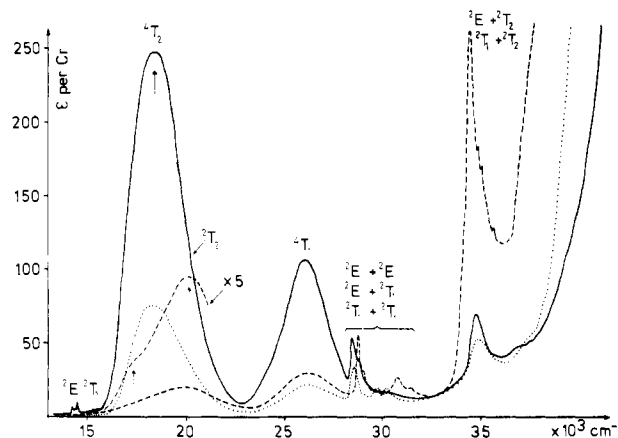


**Figure 3.** Single-crystal absorption spectrum of  $[(\text{en})_2\text{Cr}(\text{OH})_2\text{Cr}(\text{en})_2]\text{Br}_4 \cdot 2\text{H}_2\text{O}$  at 6 K. Polarizations: (—) E<sub>2</sub>, (---) E<sub>1</sub>, (····) E<sub>4</sub>, as defined in Figure 2.

by 900 and 1700  $\text{cm}^{-1}$  respectively, can be located with reasonable accuracy. The corresponding splitting of  ${}^4T_1$  is considerably smaller.

The most obvious evidence of the binuclear nature of the complex are the sharp and strong absorption bands in the near-UV. They are characteristic of exchange coupled systems<sup>14</sup> and are assigned to double excitations as indicated in Figure 3. They show very strong polarization effects. The most prominent band at 34300  $\text{cm}^{-1}$  is z polarized. The situation is different in the low-temperature spectra of  ${}^2E$ ,  ${}^2T_1$  single excitations, which are enlarged in Figure 4. x intensity dominates throughout.

The overall absorption spectra of [NH<sub>3</sub>]Cl<sub>4</sub>·4H<sub>2</sub>O and [NH<sub>3</sub>]Br<sub>4</sub>·4H<sub>2</sub>O are very similar. The bromide spectrum is reproduced in Figure 5. There are both similarities and differences to the [en]Br<sub>4</sub>·2H<sub>2</sub>O (and [en]Cl<sub>4</sub>·2H<sub>2</sub>O) spectrum. Again the spin-allowed transitions  ${}^4A_2 \rightarrow {}^4T_2$ ,  ${}^4T_1$  have dominant x components. On the other hand the splitting of  ${}^4T_2$  due to ligand field anisotropy is clearly smaller than in [en]Br<sub>4</sub>·2H<sub>2</sub>O: only two components separated by 600  $\text{cm}^{-1}$

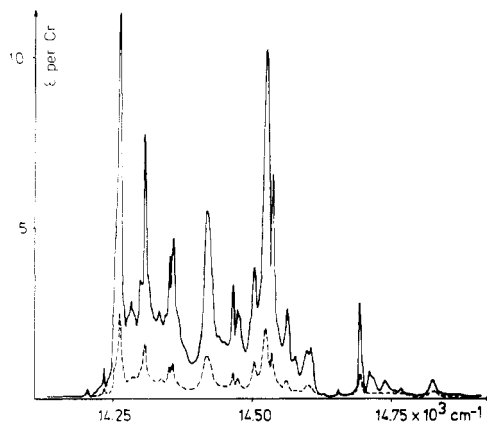


**Figure 4.** Absorption spectra at 6 K of  $[(en)_2Cr(OH)_2Cr(en)_2]Br_4 \cdot 2H_2O$  in the region of  ${}^2E$ ,  ${}^2T_1$  single excitations. Polarizations: (—)  $E_2$ , (---)  $E_1$ , as defined in Figure 2.

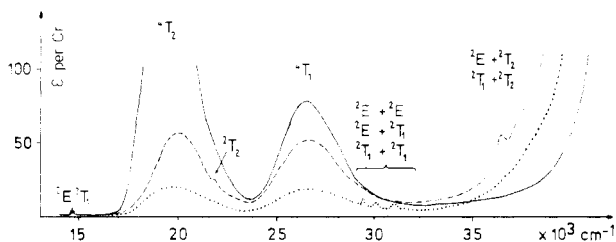


**Figure 5.** Absorption spectrum at 6 K of  $[(NH_3)_4Cr(OH)_2Cr(NH_3)_4]Br_4 \cdot 4H_2O$ . Polarizations: (—)  $R_2$ , (---)  $R_4$ , and (···)  $R_3$ , as defined in Figure 2.

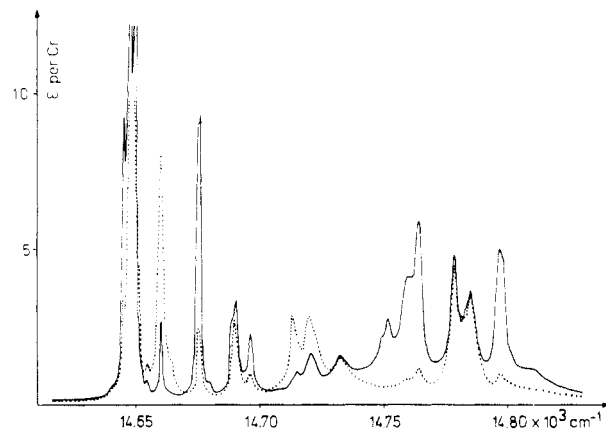


**Figure 6.** Absorption spectra at 6 K  $[(NH_3)_4Cr(OH)_2Cr(NH_3)_4]Br_4 \cdot 4H_2O$  in the region of  ${}^2E$ ,  ${}^2T_1$  single excitations. Polarizations: (—)  $R_2$  and (···)  $R_3$ , as defined in Figure 2.

can be located. The double excitations are considerably weaker, and the  ${}^2E$ ,  ${}^2T_1$  single excitations show no intensity predominance in  $x$  polarization at 5 K (Figure 6). They are even sharper than the spin-forbidden bands in  $[en]Br_4 \cdot 2H_2O$ . There is little similarity between the spectra of  $[en]$  and  $[NH_3]$  compounds in this spectral range. And there are differences between  $[NH_3]Cl_4 \cdot 4H_2O$  and  $[NH_3]Br_4 \cdot 4H_2O$  as well.

## Discussion

**(1) Spin-Allowed Transitions.** Spin-allowed transitions are known to be practically unaffected by exchange interactions in a weakly coupled system. They are best interpreted as transitions centered at a single chromium center. This general rule is nicely illustrated by our spectroscopic results. The similarity of the spin-allowed part of the absorption spectra of  $[en]$  and  $[NH_3]$  compounds is a result of the similar coordination of the chromium centers. The unusually strong dichroism in the  ${}^4A_2 \rightarrow {}^4T_2$  transition in particular is a common feature.

**Table V.** Transformation Properties and Selection Rules for Electric Dipole Transitions of a Chromium(III) Center in  $C_{2v}$  Point Symmetry<sup>a</sup>

$O_h$	$C_{2v}$	transformation	allowed ED transitions
${}^4T_{1g}$	${}^4A_2$	$R_z$	$x$ polarized
	${}^4B_1$	$R_y$	
	${}^4B_2$	$R_x$	$z$ polarized
${}^4T_{2g}$	${}^4A_2$	$xy$	$x$ polarized
	${}^4B_1$	$zx$	
	${}^4A_1$	$y^2 - z^2$	$y$ polarized
${}^4A_{2g}$	${}^4B_2$		

<sup>a</sup> Coordinate system as in Figure 1.

In all the compounds under investigation, the dimeric complex has a center of inversion as the only symmetry element.<sup>2,8,9</sup> The chromium sites have no symmetry elements. For our interpretation we use an idealized  $D_{2h}$  pair and  $C_{2v}$  single ion symmetry (Figure 1). The real structures show appreciable deviations from this approximation. Furthermore, the structures of  $[NH_3]Cl_4 \cdot 4H_2O$  and  $[NH_3]Br_4 \cdot 4H_2O$  have not yet been determined. We have to rely on the isomorphous  $[(NH_3)_4Co(OH)_2Co(NH_3)_4]Cl_4 \cdot 4H_2O$ , the published structures of which are of rather poor quality.<sup>8,9</sup> No hydrogen positions were determined. The position of the hydrogen atom at the bridging hydroxo group is of great importance to our discussion of magnetic and spectroscopic properties. In  $[(NH_3)_4Co(OH)_2Co(NH_3)_4]Cl_4 \cdot 4H_2O$  the angle between  $O \cdots Cl$  and the plane defined by I is  $63^\circ$ . The  $O \cdots Cl$  distance is  $3.24 \text{ \AA}$ , and we can assume a weak hydrogen bond  $O-H \cdots Cl$ . The great majority of hydrogen bonds of this type have angles at the hydrogen atom in the range  $150-180^\circ$ .<sup>15</sup> We conclude that in  $[NH_3]Cl_4 \cdot 4H_2O$  and  $[NH_3]Br_4 \cdot 4H_2O$  the angle between  $O-H$  and the I plane is very likely to lie between  $30$  and  $63^\circ$ .

Table V shows transformation properties and selection rules for electric dipole (ED) transitions in  $C_{2v}$  point symmetry. Both  ${}^4T_2$  and  ${}^4T_1$  are split into three components, two of which are accessible by symmetry-allowed ED transitions. From the observed temperature dependence of the spectra, the very strong  $x$  intensity is predominantly due to a static intensity mechanism, while vibronic intensity contributes in the other polarizations. We focus our attention on two aspects: (i) the unusually strong  $x$ -polarized intensity occurring in both  $[en]$  and  $[NH_3]$  compounds; (ii) the splitting of  ${}^4T_2$  into three components, which is larger in  $[en]Br_4 \cdot 2H_2O$  than in  $[NH_3]Br_4 \cdot 4H_2O$ .

Static ED intensity arises through an odd parity crystal field potential  $\hat{V}_{odd}$ . For  $C_{2v}$  point symmetry  $\hat{V}_{odd}$  has either  $T_{1u,z}$  or  $T_{2u,y}$  ( $O_h$  notation) symmetry. An effective transition dipole moment  $P_{eff}$  ( $A \rightarrow B$ ) between even parity ( $O_h$  notation) states is obtained by perturbation theory as<sup>16</sup>

$$P_{eff}(A \rightarrow B) = \sum_I \frac{\langle B | \hat{V}_{odd} | I \rangle \langle I | \hat{P} | A \rangle}{E_B - E_I} + \sum_I \frac{\langle B | \hat{P} | I \rangle \langle I | \hat{V}_{odd} | A \rangle}{E_A - E_I} \quad (1)$$

where I denotes odd parity states and  $\hat{P}$  is the electric dipole moment operator. Considering both  $\hat{P}$  and  $\hat{V}_{odd}$  to be one-electron operators, we follow an original idea by Fenske:<sup>17</sup> For an odd-parity state I to contribute to the  $A \rightarrow B$  intensity according to (1), the states A, B, and I must be made up of Slater determinants differing by no more than one orbital jump, respectively. This is a so-called configuration selection

(15) Hamilton, W. C.; Ibers, J. A. "Hydrogen Bonding in Solids"; W. A. Benjamin: Amsterdam, 1968; p 259.

(16) Sugano, S.; Tanabe, Y.; Kamimura, H. "Multiplets of Transition Metal Ions in Crystals"; Academic Press: New York, 1970; p 139.

(17) Fenske, R. F. *J. Am. Chem. Soc.* **1967**, *89*, 252.

metal orbitals      molecular orbitals      ligand orbitals

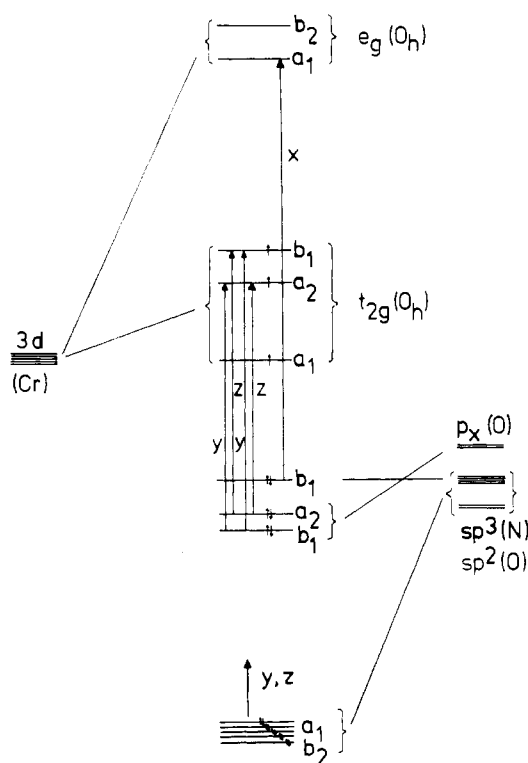


**Figure 7.** Schematic orbital diagram with symmetry-allowed one-electron charge-transfer transitions ( $C_{2v}$  symmetry notation).

rule. The most likely sources of intensity in our case are ligand to metal charge-transfer (CT) transitions. Depending on whether the acceptor orbital is  $t_{2g}$  or  $e_g$ , we get the following CT configurations ( $O_h$  notation):

$$I_1 = |\dots(t_u)^5(t_{2g})^4| \quad (2)$$

$$I_2 = |\dots(t_u)^5(t_{2g})^3(e_g)^1| \quad (3)$$

where  $t_u$  is the donor ligand molecular orbital. The ground and excited states of the d-d transitions under discussion derive, respectively, from the configurations

$$A = |\dots(t_u)^6(t_{2g})^3| \quad (4)$$

$$B = |\dots(t_u)^6(t_{2g})^2(e_g)^1| \quad (5)$$

Using the configuration selection rule, we see immediately that both  $\langle I_1 | \hat{P} | B \rangle$  and  $\langle I_1 | \hat{V}_{\text{odd}} | B \rangle$  are 0. In this one-electron approximation  $t_u \rightarrow e_g$  charge transfer is the source of intensity for the d-d transitions. For our system with a  $(t_{2g})^3$  ground configuration the intensity of the d-d transitions must not be correlated with the lowest energy charge transfer.

A schematic orbital diagram for a chromium(III) center with  $C_{2v}$  point symmetry is shown in Figure 7. Symmetry-allowed one-electron CT transitions are indicated. There is only one allowed low-energy CT transition into the  $e_g$  orbitals, and its polarization is  $x$ . This is the source of intensity of the d-d transitions according to the theoretical model. And indeed, the d-d transitions show an overwhelming predominance of  $x$  intensity in both  $[\text{en}]$  and  $[\text{NH}_3]$  compounds. We also note that, as expected, the onset of the first CT absorption between 35 000 and 40 000  $\text{cm}^{-1}$  lies at highest energy for  $x$  polarization.

Within the one-electron approximation the distribution of  $x$  intensity on the  ${}^4T_2$  and  ${}^4T_1$  transitions can be calculated and compared with experiment. The wave functions of the relevant excited states are (cf. Table V)

$${}^4A_2(T_2) = \frac{1}{2}|(y^2 - z^2)(zx)(yz)| - (3^{1/2}/2)|(y^2 - z^2)(xy)(x^2)| \quad (6)$$

$${}^4A_2(T_1) = -\frac{1}{2}|(y^2 - z^2)(xy)(x^2)| - (3^{1/2}/2)|(y^2 - z^2)(zx)(yz) \quad (7)$$

Since the intensity-providing CT transition corresponds to an electron transfer into the  $x^2$  orbital, only the Slater determinant  $|(y^2 - z^2)(xy)(x^2)|$  has to be considered in (6) and (7). The resulting intensity ratio  $I({}^4A_2(T_2))/I({}^4A_2(T_1))$  is 3. The agreement with the experimental value of 2.7 is gratifying and demonstrates the essential correctness of the theoretical model.

We next discuss the observed splittings of the  ${}^4T_2$  transitions. The fact that three components of  ${}^4T_2$  can be located in  $[\text{en}]\text{Br}_4 \cdot 2\text{H}_2\text{O}$  shows that the anisotropy of the crystal field is not axial but has a rhombic component as well. With the distortions of the coordination geometry considered, this is probably not surprising.

In the  $[\text{NH}_3]$  compounds the splitting of  ${}^4T_2$  is clearly smaller than in the corresponding  $[\text{en}]$  components. The origin of this difference is interesting. We can safely assume that a large part of the anisotropy is due to the different bonding capacities of the OH and  $\text{NH}_3(\text{en})$  ligands. Besides different  $\sigma$  bond strengths for Cr-O and Cr-N,  $\pi$  bonding is possible only for the former. From Table I we see that the hydrogen atom of the hydroxo-bridging ligand lies more or less in the I plane in the  $[\text{en}]$  compounds, while it is displaced out of this plane in the  $[\text{NH}_3]$  compounds. This means that the  $p_x$  orbital is fully available for  $\pi$  bonding to chromium in the  $[\text{en}]$  compounds, while in  $[\text{NH}_3]\text{Cl}_4 \cdot 4\text{H}_2\text{O}$  and  $[\text{NH}_3]\text{Br}_4 \cdot 4\text{H}_2\text{O}$  it is involved in the O-H  $\sigma$  bond. In the  $[\text{en}]$  case the  $\sigma$ -bonding situation at the oxygen resembles  $sp^2$  hybridization, while in the  $[\text{NH}_3]$  compounds it is more like  $sp^3$ . The contribution from OH to the ligand field is therefore much more like that of  $\text{NH}_3$  in  $[\text{NH}_3]\text{Cl}_4 \cdot 4\text{H}_2\text{O}$  and  $[\text{NH}_3]\text{Br}_4 \cdot 4\text{H}_2\text{O}$ , and thus the anisotropy and the resulting  ${}^4T_2$  splitting are smaller than that of  $[\text{en}]\text{Cl}_4 \cdot 2\text{H}_2\text{O}$  and  $[\text{en}]\text{Br}_4 \cdot 2\text{H}_2\text{O}$ . As can be seen from Table I, the different bonding at the oxygen affects not only the spectroscopic behavior but also the magnetic properties in a dramatic way. The  $p_x$  oxygen orbital quite clearly plays a dominant part in the superexchange mechanism. In the  $[\text{NH}_3]$  compounds this exchange pathway is blocked to a large extent reducing  $J$  to almost 0. Some further consequences of this are reflected in the spin-forbidden part of the absorption spectra.

**(2) Spin-Forbidden Transitions.** Spin-forbidden transitions are strongly affected by exchange interactions.<sup>14</sup> The rich fine structure observed in the region of  ${}^2E$  and  ${}^2T_1$  single excitations in the low-temperature spectra (Figures 4 and 6) is the result of exchange splittings in the ground and excited states as well as vibronic interactions. The ground-state splittings (Table I) have been obtained from the temperature dependence of intensities below 4 K. Excited-state splittings are far more difficult to evaluate, and the theoretical treatment is more complex.<sup>6</sup>

Intensities of spin-forbidden transitions may arise through the following two principal mechanisms:<sup>18</sup> (i) normal single ion mechanism, i.e., combined action of odd parity crystal field and spin-orbit coupling; (ii) pair mechanism.

Both mechanisms contribute to the intensity in our examples. The 6 K spectrum of  $[\text{en}]\text{Br}_4 \cdot 2\text{H}_2\text{O}$  in the  ${}^2E$ ,  ${}^2T_1$  region is dominated by  $x$  intensity, in close analogy to the dominance of  $x$  intensity in the  ${}^4A_2 \rightarrow {}^4T_2$  transition. This is a nice illustration of the single ion mechanism.  ${}^4A_2 \rightarrow {}^4T_2$  intensity is induced into  ${}^4A_2 \rightarrow {}^2E$ ,  ${}^2T_1$  by spin-orbit coupling. At more elevated temperatures, prominent  $y$ -polarized transitions appear, which can be interpreted as arising from a pair mech-

(18) Naito, M. *J. Phys. Soc. Jpn.* 1973, 34, 1491.

anism.<sup>6</sup> The situation is different in the 6 K spectrum of  $[\text{NH}_3]\text{Br}_4\cdot 4\text{H}_2\text{O}$ . Due to the very small ground-state splitting, all the ground levels are populated at 6 K, and as a result both mechanisms contribute to the intensity at this temperature. As a consequence, the predominance of  $x$  polarization is not as pronounced as in  $[\text{en}]\text{Br}_4\cdot 2\text{H}_2\text{O}$ .

It is interesting to compare the spectroscopic behavior of  $[\text{en}]$  and  $[\text{NH}_3]$  with that found in  $\text{Cs}_3\text{Cr}_2\text{Br}_9$ <sup>19</sup> on the one hand and  $[(\text{NH}_3)_5\text{CrOHCr}(\text{NH}_3)_5]\text{Cl}_5\cdot 3\text{H}_2\text{O}$ <sup>20</sup> on the other. In  $\text{Cs}_3\text{Cr}_2\text{Br}_9$  the chromium dimer has, as in  $[\text{en}]$  and  $[\text{NH}_3]$ , a center of inversion while in rhodo chromium chloride it has not. In the former case strong contributions to the  ${}^2\text{E}$ ,  ${}^2\text{T}_1$  intensity from a single ion mechanism have been found<sup>19</sup> while the most intense features in the pair spectrum of rhodo chromium chloride are due to a pair mechanism.<sup>20</sup> Theo-

retically the Tanabe pair mechanism is expected to be more efficient in the absence of a center of inversion.<sup>21</sup> The experimental evidence so far appears to be in good agreement with that prediction.

A detailed analysis of the spin-forbidden excitations will be published separately.<sup>6</sup>

**Acknowledgment.** We have profited from the communication of unpublished synthetic and structural information on the  $\text{NH}_3$  compounds by Johan Springborg and Erik Pedersen. This work was supported by the Swiss National Science Foundation (Grant No. 2.872-77).

**Registry No.**  $[(\text{NH}_3)_4\text{Cr}(\text{OH})_2\text{Cr}(\text{NH}_3)_4]\text{Br}_4\cdot 4\text{H}_2\text{O}$ , 67326-98-1;  $[(\text{NH}_3)_4\text{Cr}(\text{OH})_2\text{Cr}(\text{NH}_3)_4]\text{Cl}_4\cdot 4\text{H}_2\text{O}$ , 51456-44-1;  $[(\text{en})_2\text{Cr}(\text{OH})_2\text{Cr}(\text{en})_2]\text{Br}_4\cdot 2\text{H}_2\text{O}$ , 15135-03-2;  $[(\text{en})_2\text{Cr}(\text{OH})_2\text{Cr}(\text{en})_2]\text{Cl}_4\cdot 2\text{H}_2\text{O}$ , 51456-44-1;  $[(\text{NH}_3)_4\text{Cr}(\text{OH})_2\text{Cr}(\text{NH}_3)_4](\text{ClO}_4)_4\cdot 2\text{H}_2\text{O}$ , 67326-99-2.

(19) Dubicki, L.; Ferguson, J.; Harrowfield, B. *Mol. Phys.* 1977, 34, 1545.  
(20) Engel, P.; Güdel, H. U. *Inorg. Chem.* 1977, 16, 1589.

(21) Gondaira, K.; Tanabe, Y. *J. Phys. Soc. Jpn.* 1966, 21, 1527.

Contribution from the Department of Chemistry,  
Purdue University, West Lafayette, Indiana 47907

## Kinetics of Nickel(II) Glycylglycyl-L-histidine Reactions with Acids and Triethylenetetramine

CHARLES E. BANNISTER, JOHN M. T. RAYCHEBA, and DALE W. MARGERUM\*

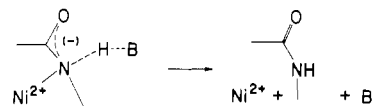
Received May 15, 1981

Dissociation of the doubly deprotonated glycylglycyl-L-histidine complex of nickel(II),  $\text{Ni}(\text{H}_2\text{GGHis})^-$ , occurs by proton-assisted and general-acid (HB) pathways. At pH 5-7 protonation of the second peptide nitrogen is the rate-limiting step as shown by contributions of  $[\text{H}^+]^2$  and  $[\text{H}^+][\text{HB}]$  terms to the rate. At high HB concentrations, the first protonation step becomes rate limiting. Below pH 5 the dissociation reaction is preceded by the formation of the outside-protonated species  $\text{Ni}(\text{H}_2\text{GGHis})\text{H}$  and  $\text{Ni}(\text{H}_2\text{GGHis})2\text{H}^+$ , in which the peptide oxygens have protonation constants of  $10^{4.3} \text{ M}^{-1}$  and  $10^{1.3} \text{ M}^{-1}$ , respectively. trien (triethylenetetramine) acts as a nucleophile in a proton-assisted pathway at pH 5-8. Comparison with the reactions of  $\text{Ni}(\text{H}_2\text{triglycinate})^-$  shows that the terminal histidyl group decreases the nucleophilic reactions of trien by more than 5 orders of magnitude. The terminal histidyl group also gives rate constants for the proton-transfer reactions of general acids which are 2-3 orders of magnitude smaller; however, the  $\text{H}_3\text{O}^+$  rate constant ( $3.0 \times 10^4 \text{ M}^{-1} \text{ s}^{-1}$ ) is only a factor of 3 smaller.

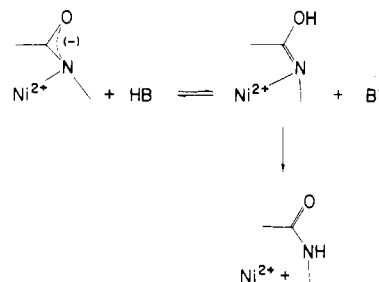
### Introduction

Kinetic studies of the acid dissociation of nickel(II) peptide complexes<sup>1-6</sup> have shown the presence of two reaction pathways. Direct peptide nitrogen protonation (Scheme I) is general-acid catalyzed. In the other reaction pathway (Scheme II), rapid peptide oxygen protonation is followed by the rate-determining metal-nitrogen bond rupture. More than one proton can add in the outside-protonation reactions. Recent work<sup>3</sup> has shown that the pathways can become mixed with general-acid attack on the outside-protonated species. In general the triply deprotonated peptide complexes  $\text{Ni}(\text{H}_3\text{G}_4)^{2-}$ ,  $\text{Ni}(\text{H}_3\text{G}_3\text{a})^-$ , and  $\text{Ni}(\text{H}_3\text{G}_4\text{a})^-$  (G, glycyl; a, amide) react by the outside-protonation pathway,<sup>2,4,5,6</sup> whereas, the doubly deprotonated peptide complex  $\text{Ni}(\text{H}_2\text{G}_3)^-$  reacts by the inside-protonation pathway.<sup>2,4</sup>

Scheme I. Inside Protonation Pathway



Scheme II. Outside Protonation Pathway



When histidine is the third amino acid in the tripeptide, the imidazole group coordinates in preference to the carboxylate group as shown for  $\text{Ni}(\text{H}_2\text{GGHis})^-$  in structure I. The present work examines the effect of this coordination on the

(1) Billo, E. J.; Margerum, D. W. *J. Am. Chem. Soc.* 1970, 92, 6811.  
(2) Paniago, E. B.; Margerum, D. W. *J. Am. Chem. Soc.* 1972, 94, 6704.  
(3) Bannister, C. E.; Margerum, D. W. *Inorg. Chem.* 1981, 20, 3149.  
(4) Bannister, C. E.; Youngblood, M. P.; Young, D. C.; Margerum, D. W., to be submitted for publication.  
(5) Raycheba, J. M. T.; Margerum, D. W. *Inorg. Chem.* 1980, 19, 497.  
(6) Raycheba, J. M. T.; Margerum, D. W. *Inorg. Chem.* 1980, 19, 837.